SCIENCE CHINA
Information Sciences

• RESEARCH PAPER •

January 2026, Vol. 69, Iss. 1, 112203:1–112203:16
https://doi.org/10.1007/s11432-024-4370-3

Observer-based fault reconstruction for continuous-time piecewise-affine systems: a novel iterative learning approach

Nuo XU[1], Yanzheng ZHU[1*], Fen WU[2] & Xinkai CHEN[3*]

[1]*College of Electrical Engineering and Automation, Shandong University of Science and Technology, Qingdao 266590, China*
[2]*Department of Mechanical and Aerospace Engineering, North Carolina State University, Raleigh NC 27695, USA*
[3]*Department of Electronic and Information Systems, Shibaura Institute of Technology, Saitama 337-8570, Japan*

Received 13 November 2024/Revised 23 December 2024/Accepted 25 March 2025/Published online 31 July 2025

Abstract In this paper, the issue of fault reconstruction is investigated for a class of continuous-time piecewise-affine (PWA) systems against actuator faults. First, to overcome the slow response issue of the conventional iterative learning law to the fault estimation error, a novel iterative accelerator and a new triggering condition, which together constitute a more efficient accelerated iterative learning law, are proposed. Then, based on the PWA iterative learning observer, the M-th accelerated iterative learning law, including a first accelerated iterative learning law as a special case, is constructed. A novel learning law updating algorithm is developed to depict the iterative procedure of fault reconstruction, the triggering process for the iterative accelerator, and the updating process. Moreover, sufficient conditions for ensuring asymptotic stability with guaranteed $\mathcal{H}_\infty$ performance are derived for the augmented PWA estimation error dynamics subject to region mismatch between the faulty system and the iterative learning observer. Finally, two examples, including a case study of a tunnel diode circuit system, are presented to fully verify the effectiveness and superiority of the proposed accelerated iterative learning method.

Keywords accelerated iterative learning law, continuous-time piecewise-affine systems, fault reconstruction, region mismatch, region-dependent Lyapunov function

Citation Xu N, Zhu Y Z, Wu F, et al. Observer-based fault reconstruction for continuous-time piecewise-affine systems: a novel iterative learning approach. Sci China Inf Sci, 2026, 69(1): 112203, https://doi.org/10.1007/s11432-024-4370-3

1 Introduction

1.1 Literature review

Industrial systems are usually subject to stringent performance requirements and demanding safety standards, and any potential fault or anomaly may cause serious damage to the normal operation of the plant [1]. In reality, faults may be produced by equipment failure, external disturbances, changes in the environment, or malicious attacks. In this context, fault reconstruction, which aims to monitor, detect, and reconstruct faults and anomalies of dynamic systems in real time, has become a crucial technology to guarantee system reliability and security. Currently, the commonly used fault reconstruction methods contain the inversion-based filter [2], the sliding mode observer [3], the polytopic learning observer [4], and the adaptive super-twisting observer [5].

Whereas, in the industrial process, a large number of modules are frequently composed of single or compound nonlinear systems, such as mechanical operation, information transmission, electric power conveyance, and other modules [6–8]. Accordingly, various accurate approximation approaches have been developed thoroughly for analyzing the nonlinear system to date. At present, several typical approximation models for nonlinear systems include the linear varying parameter system [9], the neural network system [10], and the fuzzy system [11]. The piecewise-affine (PWA) system, as a special class of hybrid systems first proposed by Hassibi and Boyd in 1998 [12], can be employed to approximate one or more sets of complex nonlinear systems. Specifically, the state space of nonlinear systems is divided into a

* Corresponding author (email: yanzhengzhu@sdust.edu.cn, chen@sic.shibaura-it.ac.jp)

series of sub-partitions, each of which can be filled via the corresponding convex polyhedral PWA region. Because of the advantage that the approximate effect of the PWA system is enhanced with the increase in the number of PWA regions, the PWA system has been widely considered in the fields of mechanics and control engineering [13–20]. In the past two decades, an increasing number of literature has reported on the modeling of complex industrial systems using the PWA approximation approach, e.g., the hydraulic wind power transfer system [21], the distributed generator in distribution grids [22], and the distributed drive electric vehicle [23].

In recent years, fault reconstruction for PWA systems has been explored extensively and intensively [24–28]. For instance, in [24], the diagnostic observer design issue of fault reconstruction is addressed for a class of PWA systems subject to the specified disturbance attenuation, and fault detectability is optimized simultaneously. In [27], the solutions for fault detection and estimation filter design are presented for linear time-invariant and PWA systems, respectively, where the hybrid Luenberger observer and its related design are presented based on quadratic boundedness. In [28], reconfigurable control is investigated for a class of continuous-time PWA systems against both the actuator and sensor faults, where both the virtual actuator and virtual sensor blocks are established to "hide" the effects of faults. However, whether the diagnostic observer, the quadratic-boundedness-based hybrid observer, or the reconfigurable control method is used, the common defect of the fault reconstruction methods proposed previously is that the convergence of fault estimation error must be ensured in finite time. If the expected estimation error cannot be reached at this time, then the fault reconstruction methods cannot self-repair the estimation error and will become invalid, which can also result in the assumption that the aforementioned methods lack intelligence. To improve the efficiency of fault reconstruction methods, more intelligent theoretical techniques need to be explored. Therefore, the gaps should be filled by developing more efficient and intelligent fault reconstruction methods for PWA systems. Furthermore, the region mismatch phenomenon may exist between the PWA system and the fault reconstruction module because of different system states. However, most of the previous research mainly focuses on fault reconstruction design and precise modeling for PWA systems in the discrete-time/continuous-time domain but ignores the region mismatch problem between different modules, which is one of the main concerns of this study.

Furthermore, as modern industrial systems continue to upgrade and exhibit more high-level intelligence, the iterative learning method is increasingly emerging as an efficient tool for addressing various challenges and problems and optimizing system performance [29–31]. The core idea of the iterative learning method is to gradually improve the performance, adaptability, and robustness of the system through repeated iterations to cope with the ever-changing environment and requirements [32, 33]. In addition, to alleviate the damage caused by system faults, the iterative-learning-based fault reconstruction has become one of the significant research directions in the field of fault estimation [34–36] and fault-tolerant control [37]. Specifically, in [34], the fault estimation issue is analyzed for a class of switched interconnected nonlinear systems by designing a novel variable-weighted iterative learning observer. In [35], the fault estimation issue is investigated for a class of Markov jump systems against sensor and nondifferentiable actuator faults. Based on the iterative learning observer, accurate fault estimation can be obtained by integrating the estimations in the iterative processes. In [37], the design issues of both Q-learning-based fault estimation and fault-tolerant iterative learning control are considered for a class of multiple-input multiple-output systems, where the controller is adjusted based on the results of both fault estimation and previous iterative learning to suppress the effect of faults. Compared with the conventional fault reconstruction methods, the iterative-learning-based fault reconstruction method has stronger adaptability and generalization capability, which is more suitable for dealing with complicated and changeable systems. However, the previous iterative learning law is usually based on the update of the estimation error, and the decreasing rate of estimation error may be slowed down step by step with the increase in iterations. Therefore, the updating efficiency of the iterative learning estimate can be impaired, and more iterations are required to achieve the desired purpose of estimation. Moreover, depending on the actual situation, the iterative learning process should be completed within a finite number of iterations. To speed up the convergence rate, the design of a more advanced iterative learning law to break the "iteration bottleneck" and avoid getting stuck in infinite iterations, which is one of the main concerns of this study, is more practical.

1.2 Contributions

Inspired by previous research, in this study, the fault reconstruction issue is concerned with a class of continuous-time PWA systems against actuator faults. First, based on the Luenberger observer, the iterative learning observer-based fault reconstruction is performed for a class of continuous-time PWA systems in the presence of region mismatch. Then, a new accelerated iterative learning law, including a learning law updating algorithm, is presented. Furthermore, the problem of asymptotic stability with guaranteed $\mathcal{H}_\infty$ performance for the augmented PWA estimation error system is addressed by employing a region-dependent Lyapunov function approach. The main contributions are listed as follows. (i) To optimize the convergence speed of the conventional iterative learning law to the fault estimation error, a novel accelerated iterative learning law is proposed by constructing a kind of iterative accelerator. Moreover, an algorithm that depicts both the learning law updating process and the iterating accelerator intervention process, in which the triggering condition is satisfied, is presented. (ii) The augmented higher-order form of the multiple accelerated iterative learning law is achieved to accelerate the convergence of fault estimation error continuously. Furthermore, a simplified accelerated iterative learning law, which can decrease computational complexity without requiring high precision, is designed in some specific cases. (iii) A new iterative-learning-based fault reconstruction observer that accommodates the mismatch of state regions between the original system and the observer is developed. Then, the region-dependent Lyapunov function is constructed to ensure asymptotic stability with the prescribed $\mathcal{H}_\infty$ performance indices for the augmented PWA estimation error dynamics.

1.3 Notations

In this study, $\mathrm{col}\{\cdot\}$ is the column vector. $\boldsymbol{R}^n$ is the vector in n-dimensional Euclidean space. $*$ and T are the transposed term in a symmetric matrix and the transpose of a matrix or vector, respectively. $\mathrm{He}\{\beta\}$ is equivalent to $\mathrm{He}\{\beta\} \triangleq \beta + \beta^{\mathrm{T}}$. I is an identity matrix with suitable dimensions. $\mathrm{ABS}(\varrho)$ is the absolute value of ϱ. $\mathcal{L}_2[0, +\infty)$ is the space of square-integrable vector functions. $\otimes$ is the Kronecker product. $\|\cdot\|$ is the Euclidean norm of vectors.

2 Problem formulation

2.1 PWA system description

Consider a class of continuous-time PWA systems with actuator faults as follows:

$$\begin{cases} \dot{x}(t) = A_i x(t) + a_i + B_i f_a(t) + D_i \omega(t), \\ y(t) = C_i x(t), \\ z(t) = E_i x(t), \ i \in \boldsymbol{I}, \end{cases} \tag{1}$$

where $x(t) \in \boldsymbol{R}^{n_x}$, $y(t) \in \boldsymbol{R}^{n_y}$, and $z(t) \in \boldsymbol{R}^{n_z}$ are the state vector, the measurement output, and the controlled output, respectively; $f_a(t)$ is the actuator faults; $\omega(t)$ is the disturbance input, which is an energy-bounded signal in $\mathcal{L}_2[0, +\infty)$; a_i is the affine term; and A_i, B_i, C_i, D_i, and E_i are system matrices with the appropriate dimensions. Subsequently, the convex polyhedral PWA region is defined as $\mathbb{R}_i \triangleq \{x \mid \mathcal{L}_i x - l_i \leqslant 0\}$, where $\mathcal{L}_i$ and l_i are constant matrices. Moreover, it holds that $\bigcup_{i \in \boldsymbol{I}} \mathbb{R}_i = \boldsymbol{R}^{n_x}$, $\mathbb{R}_i \cap \mathbb{R}_j = \emptyset$, $\forall i \neq j \in \boldsymbol{I}$. i is the index of the PWA region, and $\boldsymbol{I} \triangleq \{1, 2, \ldots, i, \ldots, \mathbb{I}\}$ is the set of all PWA region indices. Then, the set $\boldsymbol{I}$ satisfies $\boldsymbol{I} = \boldsymbol{I}_0 \cup \boldsymbol{I}_1$, where $\boldsymbol{I}_0$ and $\boldsymbol{I}_1$ are the sets containing the origin and others. As $i \in \boldsymbol{I}_0$, it yields the expression $a_i \equiv 0$. By defining $\bar{B}_i \triangleq [B_i \quad D_i]$ and $\bar{f}_a(t) \triangleq \mathrm{col}\{f_a(t) \quad \omega(t)\}$, the following expression can be derived:

$$\begin{cases} \dot{x}(t) = A_i x(t) + a_i + \bar{B}_i \bar{f}_a(t), \\ y(t) = C_i x(t), \\ z(t) = E_i x(t), \ i \in \boldsymbol{I}. \end{cases} \tag{2}$$

2.2 Fault reconstruction observer

To address the diagnostic observer design issue of fault reconstruction, consider the following Luenberger-based iterative learning observer:

$$\begin{cases} \dot{\hat{x}}^{(k)}(t) = A_j\hat{x}^{(k)}(t) + a_j + L_j(\hat{y}^{(k)}(t) - y(t)) + \bar{B}_j\hat{\bar{f}}_a^{(k)}(t), \\ \hat{y}^{(k)}(t) = C_j\hat{x}^{(k)}(t), \\ \hat{z}^{(k)}(t) = E_j\hat{x}^{(k)}(t),\ j \in \boldsymbol{I}, \end{cases} \tag{3}$$

where $\hat{x}^{(k)}(t) \in \boldsymbol{R}^{n_{\hat{x}}}$, $\hat{y}^{(k)}(t) \in \boldsymbol{R}^{n_{\hat{y}}}$, $\hat{z}^{(k)}(t) \in \boldsymbol{R}^{n_{\hat{z}}}$, and $\hat{\bar{f}}_a^{(k)}(t)$ are the estimations of $x(t)$, $y(t)$, $z(t)$, and $\bar{f}_a(t)$, respectively, k is the index for the iterations. L_j is the observer gain to be designed.

Notably, the states of the original system expressed in (2) and the fault reconstruction system expressed in (3) are different, such that the states of the two systems may be located in the distinct PWA region. Thus, a region mismatch problem between the transformed PWA system expressed in (2) and the fault reconstruction PWA iterative learning observer expressed in (3) can be detected, i.e., the index i of (2) and the index j of (3) are not the same, i.e., $i \neq j$, $\forall i, j \in \boldsymbol{I}$, which will be observed visually in Section 4.

Defining the estimation errors as $e^{(k)}(t) \triangleq \hat{x}^{(k)}(t) - x(t)$ and $e_z^{(k)}(t) \triangleq \hat{z}^{(k)}(t) - z(t)$ in accordance with (2) and (3), respectively, the following expression can be derived:

$$\dot{e}^{(k)}(t) = (A_j + L_jC_j)e^{(k)}(t) + (A_j + L_jC_j - A_i - L_jC_i)x(t) + a_j - a_i + \bar{B}_j\hat{\bar{f}}_a^{(k)}(t) - \bar{B}_i\bar{f}_a(t). \tag{4}$$

Then, an augmented state vector is defined as $\varepsilon^{(k)}(t) \triangleq \mathrm{col}\{1 \quad x(t) \quad e^{(k)}(t)\}$, and the following augmented PWA estimation error system can be obtained by combining (2) and (4):

$$\begin{cases} \dot{\varepsilon}^{(k)}(t) = \mathcal{A}_{(i,j)}\varepsilon^{(k)}(t) + \mathcal{B}_{(i,j)}\varpi^{(k)}(t), \\ e_z^{(k)}(t) = \mathcal{E}_{(i,j)}\varepsilon^{(k)}(t),\ i, j \in \boldsymbol{I}, \end{cases} \tag{5}$$

where

$$\mathcal{A}_{(i,j)} \triangleq \begin{bmatrix} 0 & 0 & 0 \\ a_i & A_i & 0 \\ a_j - a_i & \bar{A}_{(i,j)} & A_j + L_jC_j \end{bmatrix},\ \mathcal{B}_{(i,j)} \triangleq \begin{bmatrix} 0 & 0 \\ 0 & \bar{B}_i \\ \bar{B}_j & -\bar{B}_i \end{bmatrix},\ \varpi^{(k)}(t) \triangleq \begin{bmatrix} \hat{\bar{f}}_a^{(k)}(t) \\ \bar{f}_a(t) \end{bmatrix},$$
$$\mathcal{E}_{(i,j)} \triangleq [0 \quad E_j - E_i \quad E_j],\ \bar{A}_{(i,j)} \triangleq A_j - A_i + L_j(C_j - C_i).$$

2.3 Conventional iterative learning law

Generally, in accordance with [35], the conventional proportional-differential (PD)-type iterative learning law can be constructed as follows:

$$\begin{aligned} \hat{\bar{f}}_a^{(k+1)}(t) &= \hat{\bar{f}}_a^{(k)}(t) + \psi_j(\hat{y}^{(k)}(t) - y(t)) + \varphi_j(\dot{\hat{y}}^{(k)}(t) - \dot{y}(t)) \\ &= \hat{\bar{f}}_a^{(k)}(t) + \psi_j\mathcal{C}_{(i,j)}\varepsilon^{(k)}(t) + \varphi_j\mathcal{C}_{(i,j)}\dot{\varepsilon}^{(k)}(t), \end{aligned} \tag{6}$$

where ψ_j and φ_j are the gains of iterative learning law, $\forall i, j \in \boldsymbol{I}$, and $\mathcal{C}_{(i,j)} \triangleq [0 \quad C_j - C_i \quad C_j]$.

In the iterative learning law expressed in (6), both $\varepsilon^{(k)}(t)$ and $\dot{\varepsilon}^{(k)}(t)$ are the error update terms, both of which can drive the estimation $\hat{\bar{f}}_a^{(k)}(t)$ close to the augmented fault $\bar{f}_a(t)$ in real time at each iteration. However, with the increase in the number of iterations, the values of the error update terms $\varepsilon^{(k)}(t)$ and $\dot{\varepsilon}^{(k)}(t)$ become smaller gradually, which will slow down the convergence speed of the estimation $\hat{\bar{f}}_a^{(k)}(t)$ to the augmented fault $\bar{f}_a(t)$. Thus, the update efficiency of the entire iterative learning law expressed in (6) is sacrificed. As a result, the conventional method requires more iterations to reach an accurate estimation of the fault; thus, the corresponding computation time increases.

3 Main results

In this section, first, the design of a continuous region mismatch piecewise Lyapunov function is introduced. Then, based on the augmented PWA estimation error system and the conventional iterative learning law, a new M-th accelerated iterative learning method is proposed to optimize the iterative process. Furthermore, a simplified first accelerated iterative learning method, which can decrease the computational complexity without requiring high precision, is designed in some specific cases.

3.1 Boundary continuity region mismatch matrices

Following the procedures presented in [38, 39], to ensure that the piecewise Lyapunov function is continuous across the boundaries among the adjacent regions, the matrix $\Gamma_i \triangleq [r_i \quad R_i]$, $i \in \boldsymbol{I}$ with $r_i \equiv 0$ for $i \in \boldsymbol{I}_0$ is constructed to satisfy the following expression:

$$\Gamma_i \text{col}\{1 \quad x(t)\} = \Gamma_\imath \text{col}\{1 \quad x(t)\},\ x(t) \in \mathbb{R}_i \cap \mathbb{R}_\imath,\ i, \imath \in \boldsymbol{I}, \tag{7}$$

$$\Gamma_j \text{col}\{1 \quad \hat{x}^{(k)}(t)\} = \Gamma_\jmath \text{col}\{1 \quad \hat{x}^{(k)}(t)\},\ \hat{x}^{(k)}(t) \in \mathbb{R}_j \cap \mathbb{R}_\jmath,\ j, \jmath \in \boldsymbol{I}. \tag{8}$$

By combining (7) and (8), the following expression can be derived:

$$\begin{bmatrix} r_i & R_i & 0 \\ r_j & R_j & R_j \end{bmatrix} \begin{bmatrix} 1 \\ x(t) \\ e^{(k)}(t) \end{bmatrix} = \begin{bmatrix} r_\imath & R_\imath & 0 \\ r_\jmath & R_\jmath & R_\jmath \end{bmatrix} \begin{bmatrix} 1 \\ x(t) \\ e^{(k)}(t) \end{bmatrix},$$
$$x(t) \in \mathbb{R}_i \cap \mathbb{R}_\imath,\ \hat{x}^{(k)}(t) \in \mathbb{R}_j \cap \mathbb{R}_\jmath,\ i, \imath, j, \jmath \in \boldsymbol{I}. \tag{9}$$

Subsequently, the $\mathbb{S}$ procedure is employed to deal with the affine terms. By defining the matrix $\bar{\mathcal{H}}_i \triangleq [h_i \quad \mathcal{H}_i]$, $i \in \boldsymbol{I}$ with $h_i \equiv 0$ for $i \in \boldsymbol{I}_0$, the following expression can be derived:

$$\bar{\mathcal{H}}_i \text{col}\{1 \quad x(t)\} \geqslant 0,\ x(t) \in \mathbb{R}_i,\ i \in \boldsymbol{I}, \tag{10}$$

$$\bar{\mathcal{H}}_j \text{col}\{1 \quad \hat{x}^{(k)}(t)\} \geqslant 0,\ \hat{x}^{(k)}(t) \in \mathbb{R}_j,\ j \in \boldsymbol{I}. \tag{11}$$

By combining (10) and (11), the following expression can be derived:

$$\begin{bmatrix} h_i & \mathcal{H}_i & 0 \\ h_j & \mathcal{H}_j & \mathcal{H}_j \end{bmatrix} \begin{bmatrix} 1 \\ x(t) \\ e^{(k)}(t) \end{bmatrix} \geqslant 0,\ x(t) \in \mathbb{R}_i,\ \hat{x}^{(k)}(t) \in \mathbb{R}_j,\ i, j \in \boldsymbol{I}. \tag{12}$$

3.2 M-th accelerated iterative learning law

To overcome the bottleneck of the conventional iterative learning law expressed in (6) that the update of the estimated fault slows down with the increase in iterations, both a novel iterative accelerator and a trigger condition are introduced to update it, and the corresponding block diagram is shown in Figure 1. The trigger condition is defined as follows:

$$\text{ABS}(\|\hat{\hat{f}}_a^{(k+1)}(t)\| - \|\hat{\hat{f}}_a^{(k)}(t)\|) < \varsigma, \tag{13}$$

where ς is a small positive constant. As the iteration convergence rate is slower than ς, i.e., the inequality expressed in (13) holds, the iterative learning law expressed in (6) stops operating, which can be regarded as entering the "iteration bottleneck." Then, the iterative accelerator starts to intervene in the convergence rate of the iterative learning law expressed in (6) such that the iterative estimation of the fault can be accelerated. An iterative accelerator is defined to avoid falling into the first convergence bottleneck in the following:

$$\hat{\hat{f}}_a^{(1)}(t) = \psi_j \mathcal{C}_{(i,j)} \varepsilon^{(1)}(t) + \varphi_j \mathcal{C}_{(i,j)} \dot{\varepsilon}^{(1)}(t), \tag{14}$$

which is also called the first iterative accelerator. Based on the aforementioned definition of the first iterative accelerator, a novel first accelerated iterative learning law is proposed as follows:

$$\hat{\hat{f}}_a^{(k+1)}(t) = \hat{\hat{f}}_a^{(k)}(t) + \psi_j \mathcal{C}_{(i,j)} \varepsilon^{(k)}(t) + \varphi_j \mathcal{C}_{(i,j)} \dot{\varepsilon}^{(k)}(t) + \hat{\hat{f}}_a^{(1)}(t). \tag{15}$$

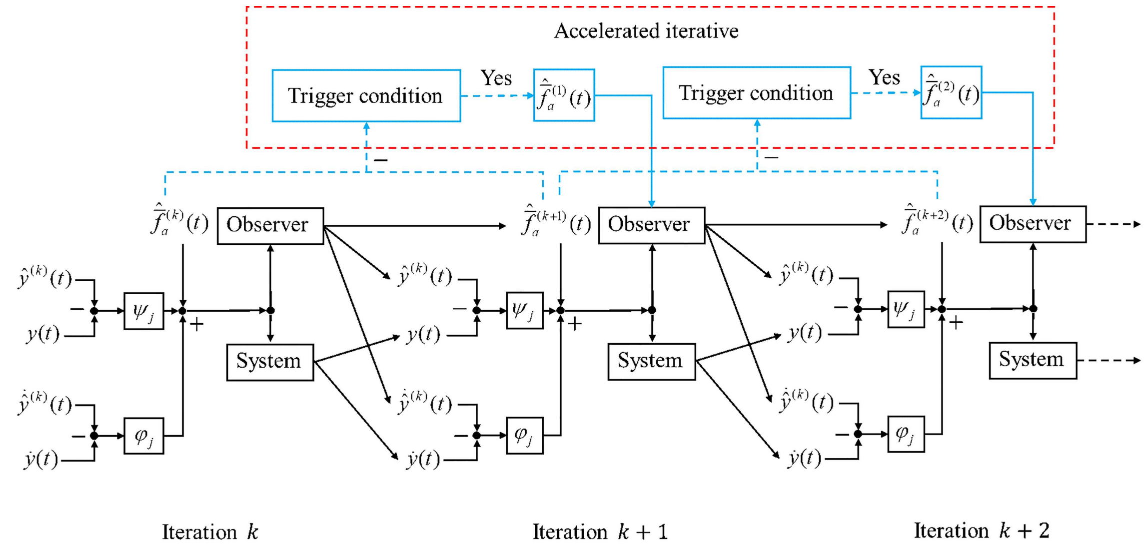

Figure 1 (Color online) Block diagram of the iterative learning law with an iterative accelerator and a trigger condition.

Remark 1. In (15), the term $\hat{\hat{f}}_a^{(1)}(t)$, which is added to the iterative learning law as a form of positive feedback, contains the information that the iterative convergence rate has slowed down to fall into the bottleneck. Then, the information gap generated from the gradually decreasing estimation error $\varepsilon^{(k)}(t)$ can be compensated such that more previous iterative data can be received for $\hat{\hat{f}}_a^{(k+1)}(t)$. Finally, the convergence rate of iterative learning is reaccelerated. Although the bottleneck of the conventional iterative learning law could be broken by the proposed first accelerated iterative learning law expressed in (15), the iteration efficiency of (15) can be still slowed down once the convergence speed of iterative estimation errors slackens again. In particular, as the trigger condition expressed in (13) is satisfied again, the first accelerated iterative learning law expressed in (15) already stops operating, which is forced into the second convergence bottleneck. As a remedy, the second iterative accelerator can be further constructed as follows:

$$\hat{\hat{f}}_a^{(2)}(t) = (\psi_j \mathcal{C}_{(i,j)}\varepsilon^{(2)}(t) + \varphi_j \mathcal{C}_{(i,j)}\dot{\varepsilon}^{(2)}(t)) + (\psi_j \mathcal{C}_{(i,j)}\varepsilon^{(1)}(t) + \varphi_j \mathcal{C}_{(i,j)}\dot{\varepsilon}^{(1)}(t)). \tag{16}$$

Moreover, based on (15) and (16), the second accelerated iterative learning law can be updated as follows:

$$\hat{\hat{f}}_a^{(k+1)}(t) = \hat{\hat{f}}_a^{(k)}(t) + \psi_j \mathcal{C}_{(i,j)}\varepsilon^{(k)}(t) + \varphi_j \mathcal{C}_{(i,j)}\dot{\varepsilon}^{(k)}(t) + \hat{\hat{f}}_a^{(1)}(t) + \hat{\hat{f}}_a^{(2)}(t). \tag{17}$$

Remark 2. Eq. (16) shows that the second iterative accelerator contains the relevant information of the first iterative accelerator. Notably, even if the "iteration bottleneck" of (6) is reached, the trigger condition will be activated again with the increase in iterations. Therefore, the acceleration can be uninterrupted through (17) based on (15) to break through the second "iteration bottleneck." By parity of reasoning, M is defined as the M-th convergence bottleneck. Then, the M-th accelerated iterative learning law with self-renewal can be obtained as follows:

$$\hat{\hat{f}}_a^{(k+1)}(t) = \hat{\hat{f}}_a^{(k)}(t) + \psi_j \mathcal{C}_{(i,j)}\varepsilon^{(k)}(t) + \varphi_j \mathcal{C}_{(i,j)}\dot{\varepsilon}^{(k)}(t) + \mathcal{F}_a^{(M)}(t), \tag{18}$$

where $\mathcal{F}_a^{(M)}(t) \triangleq \sum_{m=1}^{M} \hat{\hat{f}}_a^{(m)}(t)$. Furthermore, the following expression can be derived:

$$\begin{aligned} \hat{\hat{f}}_a^{(k+1)}(t) &= \hat{\hat{f}}_a^{(k)}(t) + \psi_j \mathcal{C}_{(i,j)}\varepsilon^{(k)}(t) + \varphi_j \mathcal{C}_{(i,j)}\dot{\varepsilon}^{(k)}(t) + \sum_{m=1}^{M} 2^{M-m}(\psi_j \mathcal{C}_{(i,j)}\varepsilon^{(m)}(t) + \varphi_j \mathcal{C}_{(i,j)}\dot{\varepsilon}^{(m)}(t)) \\ &= \hat{\hat{f}}_a^{(k)}(t) + \psi_j \mathcal{C}_{(i,j)}\varepsilon^{(k)}(t) + \varphi_j \mathcal{C}_{(i,j)}\dot{\varepsilon}^{(k)}(t) + \psi_j \mathcal{C}_{(i,j)} 2_M \Upsilon(t) + \varphi_j \mathcal{C}_{(i,j)} 2_M \dot{\Upsilon}(t), \end{aligned} \tag{19}$$

where

$$\mathcal{F}_a^{(M)}(t) \triangleq \psi_j \mathcal{C}_{(i,j)} 2_M \Upsilon(t) + \varphi_j \mathcal{C}_{(i,j)} 2_M \dot{\Upsilon}(t),$$

Algorithm 1 M-th accelerated iterative learning law updating algorithm.

Input: The iterative learning gains ψ_j and φ_j, $j \in \boldsymbol{I}$. The threshold ς.
Step 1: Initialization. Set the iteration index as $k = 0$. Set (18) as the current iterative learning law. Set $\mathcal{F}_a^{(M)}(t) = 0$ and $M = 0$.
Step 2: Operate the iterative learning law expressed in (18). Update the iteration index $k = k + 1$.
Step 3: Check whether Eq. (13) is satisfied. If yes, then update $M = M + 1$ and set $\mathcal{F}_a^{(M)}(t) = \mathcal{F}_a^{(M-1)}(t) + \hat{\bar{f}}_a^{(M)}(t)$.
Step 4: Check whether $\mathrm{ABS}(\hat{\bar{f}}_a^{(k)}(t) - \bar{f}_a(t)) \rightarrow 0$. If yes, then exit and output $\hat{\bar{f}}_a^{(k)}(t)$; else, go back to Step 2.

$$
\begin{aligned}
2_M &\triangleq [2^{M-1} \quad 2^{M-2} \quad 2^{M-3} \quad \cdots \quad 2^0],\\
\Upsilon(t) &\triangleq \mathrm{col}\{\varepsilon^{(1)}(t) \quad \varepsilon^{(2)}(t) \quad \varepsilon^{(3)}(t) \quad \cdots \quad \varepsilon^{(M)}(t)\}.
\end{aligned}
$$

Based on the M-th accelerated iterative learning law expressed in (19), the augmented M-th accelerator system can be constructed as follows:

$$
\begin{cases}
\dot{\Upsilon}(t) = (I_M \otimes \mathcal{A}_{(i,j)})\Upsilon(t) + (I_M \otimes \mathcal{B}_{(i,j)})\bar{\varpi}^{(M)}(t),\\
\bar{e}_z^{(M)}(t) = (I_M \otimes \mathcal{E}_{(i,j)})\Upsilon(t),\ i,j \in \boldsymbol{I},
\end{cases} \tag{20}
$$

where

$$
\begin{aligned}
\bar{\varpi}^{(M)}(t) &\triangleq \mathrm{col}\{\varpi^{(1)}(t) \quad \varpi^{(2)}(t) \quad \cdots \quad \varpi^{(M)}(t)\},\\
\bar{e}_z^{(M)}(t) &\triangleq \mathrm{col}\{e_z^{(1)}(t) \quad e_z^{(2)}(t) \quad e_z^{(3)}(t) \quad \cdots \quad e_z^{(M)}(t)\}.
\end{aligned}
$$

In summary, based on both the iterative accelerator expressed in (19) and the trigger condition expressed in (13), the M-th accelerated iterative learning law updating algorithm can be presented in Algorithm 1.

Remark 3. To estimate the faults accurately and decrease the estimation errors significantly, two layers of nested cycles exist in Algorithm 1. The first layer of the nested cycle is based on the variation of the iteration index k, which mainly aims to reduce the fault estimation error so that the estimation value of actuator faults can be close to its actual value. The second layer of the nested cycle is based on the variation of the acceleration index M, which mainly aims to handle the defects of the iterative learning law itself, such that the "iteration bottleneck" can be avoided.

Remark 4. The threshold ς is the switch used to start the iterative accelerator. Currently, a proper quantitative description of ς, which needs to be a constant that is small enough and greater than zero, is lacking. In the future, the specific quantization formula for the threshold ς, which will show the startup process of iterative acceleration more clearly, will be defined. Before proceeding, a new definition of asymptotic stability with guaranteed $\mathcal{H}_\infty$ performance is provided for the augmented PWA estimation error system expressed in (5) and the augmented M-th accelerator system expressed in (20).

Definition 1. Given the two scalars $\gamma > 0$ and $\gamma_M > 0$, the augmented PWA estimation error system expressed in (5) and the augmented M-th accelerator system expressed in (20) are considered to be asymptotically stable and have $\mathcal{H}_\infty$ performance indices γ and γ_M, respectively. If both of them are asymptotically stable and under the zero initial condition, then the following relationships hold for all nonzero $\varpi^{(k)}(t)$ and $\bar{\varpi}^{(M)}(t)$:

$$
\begin{aligned}
&\text{(i) } \|e_z^{(k)}(t)\| + \|\hat{\bar{f}}_a^{(k+1)}(t)\| \leqslant \gamma\|\varpi^{(k)}(t)\|,\\
&\text{(ii) } \|\bar{e}_z^{(M)}(t)\| \leqslant \gamma_M\|\bar{\varpi}^{(M)}(t)\|.
\end{aligned}
$$

In accordance with the M-th accelerated iterative learning law, sufficient conditions for ensuring asymptotic stability are derived for the augmented PWA estimation error system expressed in (5) and the augmented M-th accelerator system expressed in (20) in Theorem 1.

Theorem 1. Given the PWA system expressed in (2) and the iterative learning observer expressed in (3), if the positive definite symmetric matrix $\mathcal{G}_{(i,j)}$, symmetric matrices $P_{(i,j)}$, $Q_{(i,j)}$, and matrices $\mathcal{M}_j$, ψ_j, φ_j, $i,j \in \boldsymbol{I}$ exist, then the expressions

$$
\begin{aligned}
&\min \bar{\theta}_{i,j},\ \tilde{\theta}_{i,j},\ \text{subject to}\\
&\begin{bmatrix} \bar{\Lambda}_1 & \bar{\Lambda}_2 \\ * & \bar{\Lambda}_3 \end{bmatrix} < 0,
\end{aligned} \tag{21}
$$

$$\begin{bmatrix} -\bar{\theta}_{i,j}I & \bar{\Xi}_{i,j} \\ * & -I \end{bmatrix} < 0, \tag{22}$$

$$\begin{bmatrix} -\tilde{\theta}_{i,j}I_M & \tilde{\Xi}_{i,j} \\ * & -I_M \end{bmatrix} < 0, \tag{23}$$

$$\Gamma_{(i,j)}^{\mathrm{T}} P_{(i,j)} \Gamma_{(i,j)} > 0, \tag{24}$$

$$\Gamma_{(i,j)}^{\mathrm{T}} Q_{(i,j)} \Gamma_{(i,j)} > 0 \tag{25}$$

hold, $i, j \in \boldsymbol{I}$, where

$$\bar{\Lambda}_1 \triangleq \begin{bmatrix} \bar{\Lambda}_{1,1} & 0 & \bar{\Lambda}_{1,3} \\ * & \bar{\Lambda}_{2,2} & 0 \\ * & * & -\gamma^2 I \end{bmatrix}, \ \bar{\Lambda}_2 \triangleq \begin{bmatrix} 0 & 0 & 0 \\ 0 & \bar{\Lambda}_{2,5} & 0 \\ \bar{\Lambda}_{3,4} & \bar{\Lambda}_{3,5} & 0 \end{bmatrix}, \ \bar{\Lambda}_3 \triangleq \begin{bmatrix} -I & 0 & 0 \\ * & -\gamma_M^2 I_M & \bar{\Lambda}_{5,6} \\ * & * & -I_M \end{bmatrix},$$

with $\bar{\Lambda}_{1,1} \triangleq \mathcal{E}_{(i,j)}^{\mathrm{T}} \mathcal{E}_{(i,j)} + \mathrm{He}\{\Gamma_{(i,j)}^{\mathrm{T}} P_{(i,j)} \Gamma_{(i,j)} \mathcal{A}_{(i,j)}\} + \bar{\mathcal{H}}_{(i,j)}^{\mathrm{T}} \mathcal{G}_{(i,j)} \bar{\mathcal{H}}_{(i,j)}$, $\bar{\Lambda}_{1,3} \triangleq \Gamma_{(i,j)}^{\mathrm{T}} P_{(i,j)} \Gamma_{(i,j)} \mathcal{B}_{(i,j)}$, $\bar{\Lambda}_{2,2} \triangleq (I_M \otimes \mathcal{E}_{(i,j)})^{\mathrm{T}} (I_M \otimes \mathcal{E}_{(i,j)}) + \mathrm{He}\{\mathcal{O}_{(i,j)} (I_M \otimes \mathcal{A}_{(i,j)})\} + I_M \otimes \bar{\mathcal{H}}_{(i,j)}^{\mathrm{T}} \mathcal{G}_{(i,j)} \bar{\mathcal{H}}_{(i,j)}$, $\bar{\Lambda}_{2,5} \triangleq \mathcal{O}_{(i,j)} (I_M \otimes \mathcal{B}_{(i,j)})$, $\bar{\Lambda}_{3,4} \triangleq (\hbar + \varphi_j \mathcal{C}_{(i,j)} \mathcal{B}_{(i,j)})^{\mathrm{T}}$, $\bar{\Lambda}_{3,5} \triangleq \hbar^{\mathrm{T}} \varphi_j \mathcal{C}_{(i,j)} 2_M (I_M \otimes \mathcal{B}_{(i,j)}) + \mathcal{B}_{(i,j)}^{\mathrm{T}} \mathcal{C}_{(i,j)}^{\mathrm{T}} \mathcal{M}_j \mathcal{C}_{(i,j)} 2_M (I_M \otimes \mathcal{B}_{(i,j)})$, $\bar{\Lambda}_{5,6} \triangleq (\varphi_j \mathcal{C}_{(i,j)} 2_M (I_M \otimes \mathcal{B}_{(i,j)}))^{\mathrm{T}}$, $\bar{\Xi}_{i,j} \triangleq \psi_j \mathcal{C}_{(i,j)} + \varphi_j \mathcal{C}_{(i,j)} \mathcal{A}_{(i,j)}$, and $\tilde{\Xi}_{i,j} \triangleq \psi_j \mathcal{C}_{(i,j)} 2_M + \varphi_j \mathcal{C}_{(i,j)} 2_M (I_M \otimes \mathcal{A}_{(i,j)})$. Then, the augmented PWA estimation error system expressed in (5) and the augmented M-th accelerator system expressed in (20) are asymptotically stable with guaranteed $\mathcal{H}_\infty$ performance indices γ and γ_M, respectively.

Proof. Depending on whether the PWA region contains the origin or not, the derivations can be divided into two cases, i.e., Case I: $i, j \in \boldsymbol{I}_0$; Case II: else. Notably, Case I is the special case of Case II; therefore, only the most complex Case II is analyzed here to save space. First, a class of region-dependent Lyapunov functions is established as follows:

$$V(\varepsilon(t)) = \varepsilon^{(k)\mathrm{T}}(t) \Gamma_{(i,j)}^{\mathrm{T}} P_{(i,j)} \Gamma_{(i,j)} \varepsilon^{(k)}(t) + \Upsilon^{\mathrm{T}}(t) \mathcal{O}_{(i,j)} \Upsilon(t),$$

where

$$\mathcal{O}_{(i,j)} \triangleq I_M \otimes \Gamma_{(i,j)}^{\mathrm{T}} Q_{(i,j)} \Gamma_{(i,j)}, \ \Gamma_{(i,j)} \triangleq \begin{bmatrix} R_i & 0 \\ R_j & R_j \end{bmatrix}, \text{ if } i, j \in \boldsymbol{I}_0, \ \Gamma_{(i,j)} \triangleq \begin{bmatrix} r_i & R_i & 0 \\ r_j & R_j & R_j \end{bmatrix}, \text{ else.}$$

Letting $\mathcal{L}$ denote the infinitesimal operator, $\varpi^{(k)}(t) \equiv 0$, and $\bar{\varpi}^{(M)}(t) \equiv 0$, for $i \in \boldsymbol{I}$, $j \in \boldsymbol{I}_1$, the following expression can be derived:

$$\begin{aligned} \mathcal{L}V(\varepsilon(t)) &= \mathrm{He}\{\varepsilon^{(k)\mathrm{T}}(t) \Gamma_{(i,j)}^{\mathrm{T}} P_{(i,j)} \Gamma_{(i,j)} \mathcal{A}_{(i,j)} \varepsilon^{(k)}(t)\} + \mathrm{He}\{\Upsilon^{\mathrm{T}}(t) \mathcal{O}_{(i,j)} (I_M \otimes \mathcal{A}_{(i,j)}) \Upsilon(t)\} \\ &= \zeta^{\mathrm{T}}(t) \Xi_{(i,j)} \zeta(t), \end{aligned} \tag{26}$$

where $\zeta(t) \triangleq \mathrm{col}\{\varepsilon^{(k)}(t) \quad \Upsilon(t)\}$ and

$$\Xi_{(i,j)} \triangleq \begin{bmatrix} \Xi_{1,(i,j)} & 0 \\ * & \Xi_{2,(i,j)} \end{bmatrix},$$

with $\Xi_{1,(i,j)} \triangleq \mathrm{He}\{\Gamma_{(i,j)}^{\mathrm{T}} P_{(i,j)} \Gamma_{(i,j)} \mathcal{A}_{(i,j)}\}$ and $\Xi_{2,(i,j)} \triangleq \mathrm{He}\{\mathcal{O}_{(i,j)} (I_M \otimes \mathcal{A}_{(i,j)})\}$. To cope with the affine term, by applying the $\mathbb{S}$ procedure with matrix $\mathcal{G}_{(i,j)}$, the following expression can be derived:

$$\zeta^{\mathrm{T}}(t) \mathcal{G} \zeta(t) \triangleq \zeta^{\mathrm{T}}(t) \begin{bmatrix} \mathcal{G}_{1,1} & 0 \\ * & \mathcal{G}_{2,2} \end{bmatrix} \zeta(t), \tag{27}$$

where

$$\mathcal{G}_{1,1} \triangleq \bar{\mathcal{H}}_{(i,j)}^{\mathrm{T}} \mathcal{G}_{(i,j)} \bar{\mathcal{H}}_{(i,j)}, \ \mathcal{G}_{2,2} \triangleq I_M \otimes \bar{\mathcal{H}}_{(i,j)}^{\mathrm{T}} \mathcal{G}_{(i,j)} \bar{\mathcal{H}}_{(i,j)},$$

$$\bar{\mathcal{H}}_{(i,j)} \triangleq \begin{bmatrix} \mathcal{H}_i & 0 \\ \mathcal{H}_j & \mathcal{H}_j \end{bmatrix}, \text{ if } i,j \in \boldsymbol{I}_0,\ \bar{\mathcal{H}}_{(i,j)} \triangleq \begin{bmatrix} h_i & \mathcal{H}_i & 0 \\ h_j & \mathcal{H}_j & \mathcal{H}_j \end{bmatrix}, \text{ else.}$$

By combining (26) and (27), in accordance with [40], if Eq. (21) is satisfied, then the expression

$$\Xi_{(i,j)} + \mathcal{G} < 0 \tag{28}$$

holds, and $\mathcal{L}V(\varepsilon(t)) < 0$ holds, which indicates that the augmented PWA estimation error system expressed in (5) and the augmented M-th accelerator system expressed in (20) are asymptotically stable. Subsequently, the $\mathcal{H}_\infty$ performance of the augmented PWA estimation error system expressed in (5) and the augmented M-th accelerator system expressed in (20) is investigated. As $\varpi^{(k)}(t) \neq 0$ and $\bar{\varpi}^{(M)}(t) \neq 0$, similar to that expressed in (26), the following expression can be derived:

$$\begin{aligned} \mathcal{L}V(\varepsilon(t)) =\ & \mathrm{He}\{\varepsilon^{(k)\mathrm{T}}(t)\Gamma^{\mathrm{T}}_{(i,j)}P_{(i,j)}\Gamma_{(i,j)}(\mathcal{A}_{(i,j)}\varepsilon^{(k)}(t) + \mathcal{B}_{(i,j)}\varpi^{(k)}(t))\} + \mathrm{He}\{\Upsilon^{\mathrm{T}}(t)\mathcal{O}_{(i,j)}((I_M \\ & \otimes\mathcal{A}_{(i,j)})\Upsilon(t) + (I_M \otimes \mathcal{B}_{(i,j)})\bar{\varpi}^{(M)}(t))\}. \end{aligned} \tag{29}$$

It follows from the M-th accelerated iterative learning law expressed in (19) that

$$\begin{aligned} & \hat{\bar{f}}_a^{(k+1)\mathrm{T}}(t)\hat{\bar{f}}_a^{(k+1)}(t) \\ & = [\hbar\varpi^{(k)}(t) + \psi_j\mathcal{C}_{(i,j)}\varepsilon^{(k)}(t) + \varphi_j\mathcal{C}_{(i,j)}(\mathcal{A}_{(i,j)}\varepsilon^{(k)}(t) + \mathcal{B}_{(i,j)}\varpi^{(k)}(t)) + \psi_j\mathcal{C}_{(i,j)}2_M\Upsilon(t) \\ & \quad +\varphi_j\mathcal{C}_{(i,j)}2_M((I_M\otimes\mathcal{A}_{(i,j)})\Upsilon(t) + (I_M\otimes\mathcal{B}_{(i,j)})\bar{\varpi}^{(M)}(t))]^{\mathrm{T}}[\hbar\varpi^{(k)}(t) + \psi_j\mathcal{C}_{(i,j)}\varepsilon^{(k)}(t) \\ & \quad +\varphi_j\mathcal{C}_{(i,j)}(\mathcal{A}_{(i,j)}\varepsilon^{(k)}(t) + \mathcal{B}_{(i,j)}\varpi^{(k)}(t)) + \psi_j\mathcal{C}_{(i,j)}2_M\Upsilon(t) + \varphi_j\mathcal{C}_{(i,j)}2_M \\ & \quad \times((I_M\otimes\mathcal{A}_{(i,j)})\Upsilon(t) + (I_M\otimes\mathcal{B}_{(i,j)})\bar{\varpi}^{(M)}(t))] \\ & = \xi^{\mathrm{T}}(t)\check{\Gamma}_{(i,j)}\xi(t), \end{aligned} \tag{30}$$

where $\xi(t) \triangleq \mathrm{col}\{\varepsilon^{(k)}(t) \quad \Upsilon(t) \quad \varpi^{(k)}(t) \quad \bar{\varpi}^{(M)}(t)\}$ and

$$\begin{aligned} \check{\Gamma}_{(i,j)} \triangleq\ & \sigma_1^{\mathrm{T}}\Gamma_{1,1}\sigma_1 + \mathrm{He}\{\sigma_1^{\mathrm{T}}\Gamma_{1,2}\sigma_2 + \sigma_1^{\mathrm{T}}\Gamma_{1,3}\sigma_3 + \sigma_1^{\mathrm{T}}\Gamma_{1,4}\sigma_4\} + \sigma_2^{\mathrm{T}}\Gamma_{2,2}\sigma_2 \\ & +\mathrm{He}\{\sigma_2^{\mathrm{T}}\Gamma_{2,3}\sigma_3 + \sigma_2^{\mathrm{T}}\Gamma_{2,4}\sigma_4\} + \sigma_3^{\mathrm{T}}\Gamma_{3,3}\sigma_3 + \mathrm{He}\{\sigma_3^{\mathrm{T}}\Gamma_{3,4}\sigma_4\} + \sigma_4^{\mathrm{T}}\Gamma_{4,4}\sigma_4, \end{aligned}$$

with $\sigma_1 \triangleq [I \quad 0 \quad 0 \quad 0]$, $\sigma_2 \triangleq [0 \quad I \quad 0 \quad 0]$, $\sigma_3 \triangleq [0 \quad 0 \quad I \quad 0]$, $\sigma_4 \triangleq [0 \quad 0 \quad 0 \quad I]$, $\Gamma_{1,1} \triangleq \mathrm{He}\{\psi_j\mathcal{C}_{(i,j)} + \varphi_j\mathcal{C}_{(i,j)}\mathcal{A}_{(i,j)}\}$, $\Gamma_{1,2} \triangleq (\psi_j\mathcal{C}_{(i,j)}+\varphi_j\mathcal{C}_{(i,j)}\mathcal{A}_{(i,j)})^{\mathrm{T}}(\psi_j\mathcal{C}_{(i,j)}2_M+\varphi_j\mathcal{C}_{(i,j)}2_M\times(I_M\otimes\mathcal{A}_{(i,j)}))$, $\Gamma_{1,3} \triangleq (\psi_j\mathcal{C}_{(i,j)}+\varphi_j\mathcal{C}_{(i,j)}\mathcal{A}_{(i,j)})^{\mathrm{T}} \times (\hbar + \varphi_j\mathcal{C}_{(i,j)}\mathcal{B}_{(i,j)})$, $\Gamma_{1,4} \triangleq (\psi_j\mathcal{C}_{(i,j)} + \varphi_j\mathcal{C}_{(i,j)}\mathcal{A}_{(i,j)})^{\mathrm{T}}(\varphi_j\mathcal{C}_{(i,j)}2_M(I_M\otimes\mathcal{B}_{(i,j)}))$, $\Gamma_{2,2} \triangleq \mathrm{He}\{\psi_j\mathcal{C}_{(i,j)}2_M+\varphi_j\mathcal{C}_{(i,j)}2_M(I_M\otimes\mathcal{A}_{(i,j)})\}$, $\Gamma_{2,3} \triangleq (\psi_j\mathcal{C}_{(i,j)}2_M+\varphi_j\mathcal{C}_{(i,j)}2_M(I_M\otimes\mathcal{A}_{(i,j)}))^{\mathrm{T}}(\hbar+\varphi_j\mathcal{C}_{(i,j)}\mathcal{B}_{(i,j)})$, $\Gamma_{2,4} \triangleq (\psi_j\mathcal{C}_{(i,j)}2_M + \varphi_j\mathcal{C}_{(i,j)}2_M(I_M\otimes\mathcal{A}_{(i,j)}))^{\mathrm{T}}(\varphi_j\mathcal{C}_{(i,j)}2_M(I_M\otimes\mathcal{B}_{(i,j)}))$, $\Gamma_{3,3} \triangleq \mathrm{He}\{\hbar + \varphi_j\mathcal{C}_{(i,j)}\mathcal{B}_{(i,j)}\}$, $\Gamma_{3,4} \triangleq (\hbar + \varphi_j\mathcal{C}_{(i,j)}\mathcal{B}_{(i,j)})^{\mathrm{T}}(\varphi_j\mathcal{C}_{(i,j)}2_M(I_M\otimes\mathcal{B}_{(i,j)}))$, and $\Gamma_{4,4} \triangleq \mathrm{He}\{\varphi_j\mathcal{C}_{(i,j)}2_M(I_M\otimes\mathcal{B}_{(i,j)})\}$. Based on (29) and (30), under the zero initial condition, the $\mathcal{H}_\infty$ performance indices for the augmented PWA estimation error system expressed in (5) and the augmented M-th accelerator system expressed in (20) can be established, respectively, as follows:

$$\begin{aligned} \boldsymbol{J}_1 &= \int_0^\infty (e_z^{(k)\mathrm{T}}(t)e_z^{(k)}(t) + \hat{\bar{f}}_a^{(k+1)\mathrm{T}}(t)\hat{\bar{f}}_a^{(k+1)}(t) - \gamma^2\varpi^{(k)\mathrm{T}}(t)\varpi^{(k)}(t))\mathrm{d}t, \\ \boldsymbol{J}_2 &= \int_0^\infty (\bar{e}_z^{(M)\mathrm{T}}(t)\bar{e}_z^{(M)}(t) - \gamma_M^2\bar{\varpi}^{(M)\mathrm{T}}(t)\bar{\varpi}^{(M)}(t))\mathrm{d}t. \end{aligned}$$

By combining these two performance index functions, the following expression can be derived:

$$\begin{aligned} \boldsymbol{J} &= \boldsymbol{J}_1 + \boldsymbol{J}_2 \\ &= \int_0^\infty (e_z^{(k)\mathrm{T}}(t)e_z^{(k)}(t) + \hat{\bar{f}}_a^{(k+1)\mathrm{T}}(t)\hat{\bar{f}}_a^{(k+1)}(t) + \bar{e}_z^{(M)\mathrm{T}}(t)\bar{e}_z^{(M)}(t) - \gamma^2\varpi^{(k)\mathrm{T}}(t)\varpi^{(k)}(t) \\ &\quad -\gamma_M^2\bar{\varpi}^{(M)\mathrm{T}}(t)\bar{\varpi}^{(M)}(t))\mathrm{d}t \\ &\leqslant \int_0^\infty (e_z^{(k)\mathrm{T}}(t)e_z^{(k)}(t) + \hat{\bar{f}}_a^{(k+1)\mathrm{T}}(t)\hat{\bar{f}}_a^{(k+1)}(t) + \bar{e}_z^{(M)\mathrm{T}}(t)\bar{e}_z^{(M)}(t) - \gamma^2\varpi^{(k)\mathrm{T}}(t)\varpi^{(k)}(t) \end{aligned}$$

$$-\gamma_M^2 \bar{\varpi}^{(M)\mathrm{T}}(t)\bar{\varpi}^{(M)}(t) + \mathcal{L}V(\varepsilon(t)))\mathrm{d}t$$
$$= \int_0^\infty \xi^{\mathrm{T}}(t)(\check{\Gamma}_{(i,j)} + \bar{\Gamma}_{(i,j)})\xi(t)\mathrm{d}t, \tag{31}$$

where

$$\bar{\Gamma}_{(i,j)} \triangleq \sigma_1^{\mathrm{T}}\bar{\Gamma}_{1,1}\sigma_1 + \mathrm{He}\{\sigma_1^{\mathrm{T}}\bar{\Gamma}_{1,3}\sigma_3\} + \sigma_2^{\mathrm{T}}\bar{\Gamma}_{2,2}\sigma_2 + \mathrm{He}\{\sigma_2^{\mathrm{T}}\bar{\Gamma}_{2,4}\sigma_4\} - \sigma_3^{\mathrm{T}}\gamma^2 I\sigma_3 - \sigma_4^{\mathrm{T}}\gamma_M^2 I_M\sigma_4,$$

with $\bar{\Gamma}_{1,1} \triangleq \mathcal{E}_{(i,j)}^{\mathrm{T}}\mathcal{E}_{(i,j)} + \mathrm{He}\{\Gamma_{(i,j)}^{\mathrm{T}}P_{(i,j)}\Gamma_{(i,j)}\mathcal{A}_{(i,j)}\}$, $\bar{\Gamma}_{1,3} \triangleq \Gamma_{(i,j)}^{\mathrm{T}}P_{(i,j)}\Gamma_{(i,j)}\mathcal{B}_{(i,j)}$, $\bar{\Gamma}_{2,2} \triangleq (I_M \otimes \mathcal{E}_{(i,j)})^{\mathrm{T}}(I_M \otimes \mathcal{E}_{(i,j)}) + \mathrm{He}\{\mathcal{O}_{(i,j)}(I_M \otimes \mathcal{A}_{(i,j)})\}$, and $\bar{\Gamma}_{2,4} \triangleq \mathcal{O}_{(i,j)}(I_M \otimes \mathcal{B}_{(i,j)})$. To cope with the affine term, by applying the $\mathbb{S}$ procedure with matrix $\mathcal{G}_{(i,j)}$, the following expression can be derived:

$$\xi^{\mathrm{T}}(t)\mathcal{H}\xi(t) \triangleq \xi^{\mathrm{T}}(t)(\sigma_1^{\mathrm{T}}\bar{\mathcal{H}}_{(i,j)}^{\mathrm{T}}\mathcal{G}_{(i,j)}\bar{\mathcal{H}}_{(i,j)}\sigma_1 + \sigma_2^{\mathrm{T}}I_M \otimes \bar{\mathcal{H}}_{(i,j)}^{\mathrm{T}}\mathcal{G}_{(i,j)}\bar{\mathcal{H}}_{(i,j)}\sigma_2)\xi(t). \tag{32}$$

By combining (31) and (32), the following expression can be derived:

$$\boldsymbol{J} = \int_0^\infty \xi^{\mathrm{T}}(t)(\check{\Gamma}_{(i,j)} + \bar{\Gamma}_{(i,j)} + \mathcal{H})\xi(t)\mathrm{d}t. \tag{33}$$

Notably, Eq. (33) is nonconvex; therefore, a fault reconstruction method is proposed to cope with this nonconvexity problem as follows:

$$\psi_j\mathcal{C}_{(i,j)} = -\varphi_j\mathcal{C}_{(i,j)}\mathcal{A}_{(i,j)}, \tag{34}$$
$$\psi_j\mathcal{C}_{(i,j)}2_M = -\varphi_j\mathcal{C}_{(i,j)}2_M(I_M \otimes \mathcal{A}_{(i,j)}). \tag{35}$$

By employing the technique presented in [41], Eqs. (34) and (35) can be transformed, respectively, as follows:

$$\mathrm{Trace}((\psi_j\mathcal{C}_{(i,j)} + \varphi_j\mathcal{C}_{(i,j)}\mathcal{A}_{(i,j)})^{\mathrm{T}}(\psi_j\mathcal{C}_{(i,j)} + \varphi_j\mathcal{C}_{(i,j)}\mathcal{A}_{(i,j)})) = 0,$$

and

$$\mathrm{Trace}((\psi_j\mathcal{C}_{(i,j)}2_M + \varphi_j\mathcal{C}_{(i,j)}2_M(I_M \otimes \mathcal{A}_{(i,j)}))^{\mathrm{T}}(\psi_j\mathcal{C}_{(i,j)}2_M + \varphi_j\mathcal{C}_{(i,j)}2_M(I_M \otimes \mathcal{A}_{(i,j)}))) = 0.$$

Then, the expressions

$$(\psi_j\mathcal{C}_{(i,j)} + \varphi_j\mathcal{C}_{(i,j)}\mathcal{A}_{(i,j)})^{\mathrm{T}}(\psi_j\mathcal{C}_{(i,j)} + \varphi_j\mathcal{C}_{(i,j)}\mathcal{A}_{(i,j)}) < \bar{\theta}_{i,j}I \tag{36}$$

and

$$(\psi_j\mathcal{C}_{(i,j)}2_M + \varphi_j\mathcal{C}_{(i,j)}2_M(I_M \otimes \mathcal{A}_{(i,j)}))^{\mathrm{T}}(\psi_j\mathcal{C}_{(i,j)}2_M + \varphi_j\mathcal{C}_{(i,j)}2_M(I_M \otimes \mathcal{A}_{(i,j)})) < \tilde{\theta}_{i,j}I_M \tag{37}$$

hold, where both $\bar{\theta}_{i,j}$ and $\tilde{\theta}_{i,j}$ are two small positive scalars. By applying the Schur complement, the inequalities expressed in (36) and (37) can be converted into the minimization issues expressed in (22) and (23), respectively. In summary, the following expression can be derived:

$$\boldsymbol{J} = \int_0^\infty \xi^{\mathrm{T}}(t)\Omega_{(i,j)}\xi(t)\mathrm{d}t, \tag{38}$$

where $\Omega_{(i,j)}$ can be obtained from (21). According to Definition 1, if Eq. (21) is satisfied, then $\boldsymbol{J} < 0$ holds, which indicates that the augmented PWA estimation error system expressed in (5) and the augmented M-th accelerator system expressed in (20) are asymptotically stable with the guaranteed $\mathcal{H}_\infty$ performance indices γ and γ_M, respectively. The proof is completed.

3.3 First accelerated iterative learning law

Although M-th accelerated iterative learning method can considerably accelerate the convergence rate of iterative errors, the computational complexity of the iterative learning law will increase as accelerators are inserted to accelerate continuously. In some cases, the first accelerated iterative learning law expressed in (15) is only required to satisfactorily achieve the convergence goal. Therefore, a simplified method (or

Algorithm 2 First accelerated iterative learning law updating algorithm.

Input: The iterative learning gains ψ_j and φ_j, $j \in \boldsymbol{I}$. The threshold ς.
Step 1: Initialization. Set the iteration index as $k = 0$. Set (6) as the current iterative learning law.
Step 2: Operate the iterative learning law expressed in (6). Update the iteration index $k = k + 1$.
Step 3: Check whether Eq. (13) is satisfied. If yes, then update and set first accelerated iterative learning law expressed in (15).
Step 4: Operate the new iterative learning law expressed in (15). Update the iteration index $k = k + 1$.
Step 5: Check whether $\mathrm{ABS}(\hat{\bar{f}}_a^{(k)}(t) - \bar{f}_a(t)) \to 0$. If yes, then exit and output $\hat{\bar{f}}_a^{(k)}(t)$; else, go back to Step 4.

a special case) is developed for the M-th accelerated iterative learning law expressed in (19), i.e., the iterative learning law is accelerated only once. In accordance with the first accelerated iterative learning law expressed in (15), the first accelerator system can be constructed as follows:

$$\begin{cases} \dot{\varepsilon}^{(1)}(t) = \mathcal{A}_{(i,j)}\varepsilon^{(1)}(t) + \mathcal{B}_{(i,j)}\varpi^{(1)}(t), \\ e_z^{(1)}(t) = \mathcal{E}_{(i,j)}\varepsilon^{(1)}(t),\ i,j \in \boldsymbol{I}. \end{cases} \tag{39}$$

Then, based on both the iterative accelerator expressed in (14) and the trigger condition expressed in (13), the first accelerated iterative learning law updating algorithm can be obtained using Algorithm 2.

Remark 5. Two judgment conditions exist in Algorithm 2, i.e., the trigger condition and the satisfactory estimation condition. The trigger condition is positioned before the satisfactory condition because, generally, the value of the former exceeds that of the latter, and the response speed of the iterative learning law is slowed down gradually with the increase in iterations. Thus, the threshold of the trigger condition is bounded before the satisfactory estimation error is met. In accordance with the first accelerated iterative learning law, sufficient conditions for ensuring asymptotic stability with the prescribed $\mathcal{H}_\infty$ performance indices are derived for the augmented PWA estimation error system expressed in (5) and the first accelerator system expressed in (39).

Corollary 1. Given the PWA system expressed in (2) and the iterative learning observer expressed in (3), if the positive definite symmetric matrix $\mathcal{G}_{(i,j)}$, symmetric matrices $P_{(i,j)}$, $Q_{(i,j)}$, and matrices $\mathcal{M}_j$, ψ_j, φ_j, $i,j \in \boldsymbol{I}$ exist, then the expressions

$$\min \theta_{i,j},\ \text{subject to}$$

$$\begin{bmatrix} \Lambda_1 & \Lambda_2 \\ * & \Lambda_3 \end{bmatrix} < 0, \tag{40}$$

$$\begin{bmatrix} -\theta_{i,j} I & \Xi_{i,j} \\ * & -I \end{bmatrix} < 0, \tag{41}$$

$$\Gamma_{(i,j)}^{\mathrm{T}} P_{(i,j)} \Gamma_{(i,j)} > 0, \tag{42}$$

$$\Gamma_{(i,j)}^{\mathrm{T}} Q_{(i,j)} \Gamma_{(i,j)} > 0 \tag{43}$$

hold, $i,j \in \boldsymbol{I}$, where

$$\Lambda_1 \triangleq \begin{bmatrix} \Lambda_{1,1} & 0 & \Lambda_{1,3} \\ * & \Lambda_{2,2} & 0 \\ * & * & -\gamma^2 I \end{bmatrix},\ \Lambda_2 \triangleq \begin{bmatrix} 0 & 0 & 0 \\ 0 & \Lambda_{2,5} & 0 \\ \Lambda_{3,4} & \Lambda_{3,5} & 0 \end{bmatrix},\ \Lambda_3 \triangleq \begin{bmatrix} -I & 0 & 0 \\ * & -\gamma_{(1)}^2 I_{(1)} & \Lambda_{5,6} \\ * & * & -I_{(1)} \end{bmatrix},$$

with $\Lambda_{1,1} \triangleq \mathcal{E}_{(i,j)}^{\mathrm{T}}\mathcal{E}_{(i,j)} + \mathrm{He}\{\Gamma_{(i,j)}^{\mathrm{T}} P_{(i,j)} \Gamma_{(i,j)} \mathcal{A}_{(i,j)}\} + \bar{\mathcal{H}}_{(i,j)}^{\mathrm{T}} \mathcal{G}_{(i,j)} \bar{\mathcal{H}}_{(i,j)}$, $\Lambda_{1,3} \triangleq \Gamma_{(i,j)}^{\mathrm{T}} P_{(i,j)} \Gamma_{(i,j)} \mathcal{B}_{(i,j)}$, $\Lambda_{2,2} \triangleq \mathcal{E}_{(i,j)}^{\mathrm{T}}\mathcal{E}_{(i,j)} + \mathrm{He}\{\Gamma_{(i,j)}^{\mathrm{T}} Q_{(i,j)} \Gamma_{(i,j)} \mathcal{A}_{(i,j)}\} + \bar{\mathcal{H}}_{(i,j)}^{\mathrm{T}} \mathcal{G}_{(i,j)} \bar{\mathcal{H}}_{(i,j)}$, $\Lambda_{2,5} \triangleq \Gamma_{(i,j)}^{\mathrm{T}} Q_{(i,j)} \Gamma_{(i,j)} \mathcal{B}_{(i,j)}$, $\Lambda_{3,4} \triangleq (\hbar + \varphi_j \mathcal{C}_{(i,j)} \mathcal{B}_{(i,j)})^{\mathrm{T}}$, $\Lambda_{3,5} \triangleq \hbar^{\mathrm{T}} \varphi_j \mathcal{C}_{(i,j)} \mathcal{B}_{(i,j)} + \mathcal{B}_{(i,j)}^{\mathrm{T}} \mathcal{C}_{(i,j)}^{\mathrm{T}} \mathcal{M}_j \mathcal{C}_{(i,j)} \mathcal{B}_{(i,j)}$, $\Lambda_{5,6} \triangleq (\varphi_j \mathcal{C}_{(i,j)} \mathcal{B}_{(i,j)})^{\mathrm{T}}$, and $\Xi_{i,j} \triangleq \psi_j \mathcal{C}_{(i,j)} + \varphi_j \mathcal{C}_{(i,j)} \mathcal{A}_{(i,j)}$. Then, the augmented PWA estimation error system expressed in (5) and the first accelerator system expressed in (39) are asymptotically stable with $\mathcal{H}_\infty$ performance indices γ, $\gamma_{(1)}$, respectively.

Proof. Similar to the proof of Theorem 1, Corollary 1 can also be divided into two cases, i.e., Case I: $i,j \in \boldsymbol{I}_0$; Case II: else. Here, only the most complex Case II is analyzed to save space. First, a class of region-dependent Lyapunov functions is constructed as follows:

$$V(\varepsilon(t)) = \varepsilon^{(k)\mathrm{T}}(t) \Gamma_{(i,j)}^{\mathrm{T}} P_{(i,j)} \Gamma_{(i,j)} \varepsilon^{(k)}(t) + \varepsilon^{(1)\mathrm{T}}(t) \Gamma_{(i,j)}^{\mathrm{T}} Q_{(i,j)} \Gamma_{(i,j)} \varepsilon^{(1)}(t),$$

where $\Gamma_{(i,j)}$ is given in Theorem 1. Based on the first accelerated iterative learning law expressed in (15), the augmented term is defined as follows:

$$\xi(t) \triangleq \text{col}\{\varepsilon^{(k)}(t) \quad \varepsilon^{(1)}(t) \quad \varpi^{(k)}(t) \quad \varpi^{(1)}(t)\}.$$

To cope with the nonconvexity issue, similar to the proof of Theorem 1, the fault reconstruction method can be used, and the following relations are obtained:

$$\psi_j \mathcal{C}_{(i,j)} = -\varphi_j \mathcal{C}_{(i,j)} \mathcal{A}_{(i,j)}. \tag{44}$$

By employing the technique presented in [41], Eq. (44) can be transformed as follows:

$$\text{Trace}((\psi_j \mathcal{C}_{(i,j)} + \varphi_j \mathcal{C}_{(i,j)} \mathcal{A}_{(i,j)})^{\mathrm{T}} (\psi_j \mathcal{C}_{(i,j)} + \varphi_j \mathcal{C}_{(i,j)} \mathcal{A}_{(i,j)})) = 0.$$

Then, the following expression can be derived:

$$(\psi_j \mathcal{C}_{(i,j)} + \varphi_j \mathcal{C}_{(i,j)} \mathcal{A}_{(i,j)})^{\mathrm{T}} (\psi_j \mathcal{C}_{(i,j)} + \varphi_j \mathcal{C}_{(i,j)} \mathcal{A}_{(i,j)}) < \theta_{i,j} I, \tag{45}$$

where $\theta_{i,j}$ is a small positive scalar. By applying the Schur complement, Eq. (45) can be converted into the inequality expressed in (41). The rest of the proof follows directly from the proof of Theorem 1, thereby completing the proof.

4 Illustrative examples

In this section, first, a numerical example is developed to demonstrate the effectiveness and advantage of the proposed fault reconstruction PWA iterative learning observer design approach and the accelerated iterative learning strategy. Then, a tunnel diode circuit system is employed to verify the practicability of the proposed accelerated iterative learning strategy.

Example 1. Given the continuous-time PWA system expressed in (1) with four regions, the system matrices are expressed as follows:

$$A_1 = \varsigma \begin{bmatrix} 0 & 0.37 \\ -0.73 & -0.72 \end{bmatrix}, \ A_2 = \varsigma \begin{bmatrix} 0 & 0.25 \\ -0.73 & -1.02 \end{bmatrix}, \ A_3 = \varsigma \begin{bmatrix} 0 & 0.72 \\ -0.73 & -0.88 \end{bmatrix}, \ A_4 = \varsigma \begin{bmatrix} 0 & 0.17 \\ -0.73 & -0.81 \end{bmatrix},$$
$$a_1 = \varsigma \begin{bmatrix} 0 \\ 0 \end{bmatrix}, a_2 = \varsigma \begin{bmatrix} -0.93 \\ 0.56 \end{bmatrix}, a_3 = \varsigma \begin{bmatrix} -0.20 \\ -0.64 \end{bmatrix}, \ a_4 = \varsigma \begin{bmatrix} 0.87 \\ -0.39 \end{bmatrix}, \ B_i = \begin{bmatrix} 1 \\ 1 \end{bmatrix}, \ C_i = \begin{bmatrix} 1 & 1 \end{bmatrix}, \ D_i = \begin{bmatrix} 1 \\ -1 \end{bmatrix},$$
$$E_i = \begin{bmatrix} 1 & -1 \end{bmatrix},$$

where $i \in \boldsymbol{I}$, $\boldsymbol{I} = \{1, 2, 3, 4\}$ with four regions, i.e.,

$$\mathcal{L}_1 = \begin{bmatrix} -3 & 2 \\ 2 & 1 \\ -1 & -4 \end{bmatrix}, l_1 = \begin{bmatrix} 60 \\ 30 \\ 90 \end{bmatrix}, \mathcal{L}_2 = \begin{bmatrix} 3 & -2 \end{bmatrix}, l_2 = -60, \mathcal{L}_3 = \begin{bmatrix} -2 & -1 \end{bmatrix}, l_3 = -30, \mathcal{L}_4 = \begin{bmatrix} 1 & 4 \end{bmatrix}, l_4 = -90.$$

From Theorem 1 associated with Algorithm 1, by setting $\varsigma = 4$, the trajectories of the original system state and the observer state in different PWA regions are plotted in Figure 2(a), which shows that the two states are located in two different PWA regions in the initial stage and remain at different PWA regions in the subsequent operation process, i.e., the original system state passes through PWA regions $\mathbb{R}_1$, $\mathbb{R}_2$, and $\mathbb{R}_1$ in sequence, whereas the observer state passes through PWA regions $\mathbb{R}_4$ and $\mathbb{R}_1$ in sequence. Notably, the original system can be estimated accurately by the designed PWA iterative learning observer, even under the presence of region mismatch. In addition, the trajectories of actuator faults and the conventional-based, first-accelerated-based, second-accelerated-based, and third-accelerated-based fault reconstructions are plotted in Figure 2(b). With the continued operation of the iterative accelerator, the "iteration bottleneck" of the slow estimation is broken through consecutively, and the estimation of the actuator fault can be obtained accurately via the PWA iterative learning observer after three consecutive accelerations.

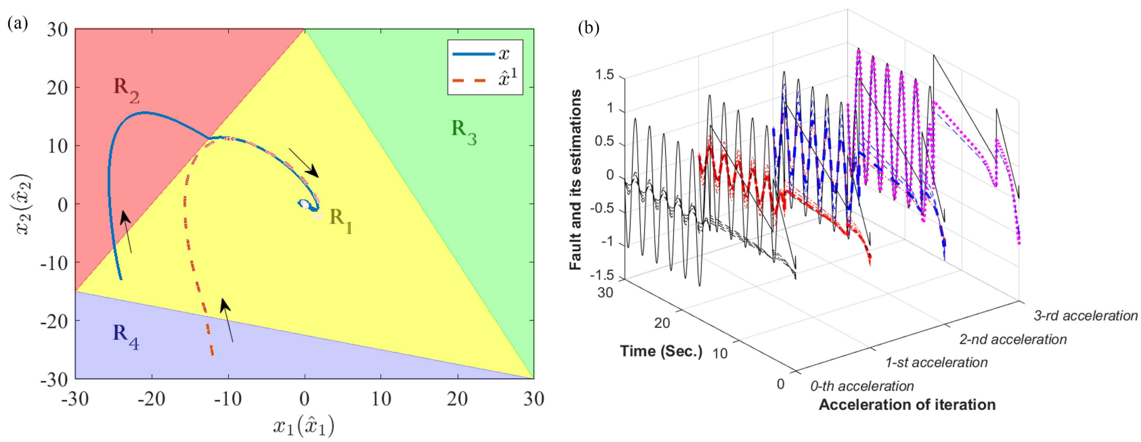

Figure 2 (Color online) Trajectories of $x(t)$, $\hat{x}^{(k)}(t)$, and fault reconstructions in Example 1. (a) Trajectories of $x(t)$ and $\hat{x}^{(k)}(t)$ in different PWA regions; (b) trajectories of multiple acceleration fault reconstructions.

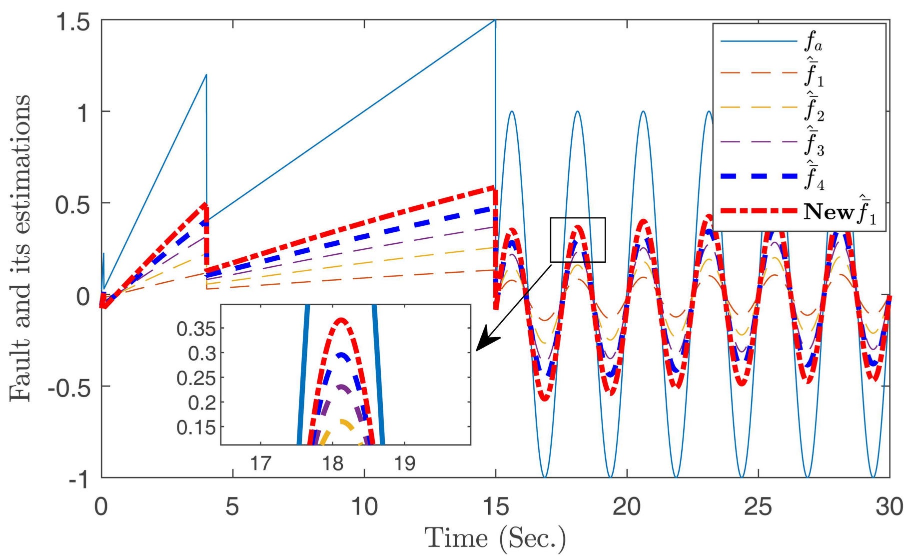

Figure 3 (Color online) Comparison between the conventional iterative learning law (blue) and the first accelerated iterative learning law (red) for fault reconstruction in Example 1.

Furthermore, from Corollary 1 associated with Algorithm 2, by setting $\varsigma = 1$, the trajectories of actuator faults and the conventional-based and first-accelerated-based fault reconstructions are plotted in Figure 3 under the initial condition $f_a(0) = 0$. Figure 3 shows that, in the first three iterations, the convergence speed of conventional fault reconstruction slows down gradually. Starting from the fourth iteration, the convergence amplitude of the first-accelerated-based fault reconstruction (red) is significantly higher than that of the conventional-based fault reconstruction (blue), which indicates that the "iteration bottleneck" can be broken by the first accelerated iterative learning law; hence, the convergence speed can be improved.

Example 2. Consider the tunnel diode circuit system [42] whose characteristics can be described as follows:

$$\begin{cases} \dot{\mathcal{V}}_c(t) = C^{-1}(-\varrho_1 \mathcal{V}_c(t) - \varrho_2 \mathcal{V}_c(t)^3 + \mathcal{I}_L(t)), \\ \dot{\mathcal{I}}_L(t) = L^{-1}(-\mathcal{V}_c(t) - R\mathcal{I}_L(t) + \omega(t)), \end{cases} \tag{46}$$

where $\mathcal{V}_c(t)$ is the voltage across the capacitor, $\mathcal{I}_L(t)$ is the current flowing through the inductor, R is the resistor, C is the capacitor, L is the inductor, $\omega(t)$ is the disturbance, and ϱ_1 and ϱ_2 are the scalars. By approximating (46) using the PWA system model expressed in (1) with three regions, i.e., $\mathbb{R}_1 \triangleq \{\mathcal{V}_c(t) \mid -4 \leqslant \mathcal{V}_c(t) < -1\}$, $\mathbb{R}_2 \triangleq \{\mathcal{V}_c(t) \mid -1 \leqslant \mathcal{V}_c(t) \leqslant 1\}$, and $\mathbb{R}_3 \triangleq \{\mathcal{V}_c(t) \mid 1 < \mathcal{V}_c(t) \leqslant 4\}$, and by defining $x(t) = \mathrm{col}\{\mathcal{V}_c(t)\ \mathcal{I}_L(t)\}$, $R = 5\Omega$, $C = 0.05$F, $L = 0.2$H, $\varrho_1 = 0.002$, and $\varrho_2 = 0.01$, the

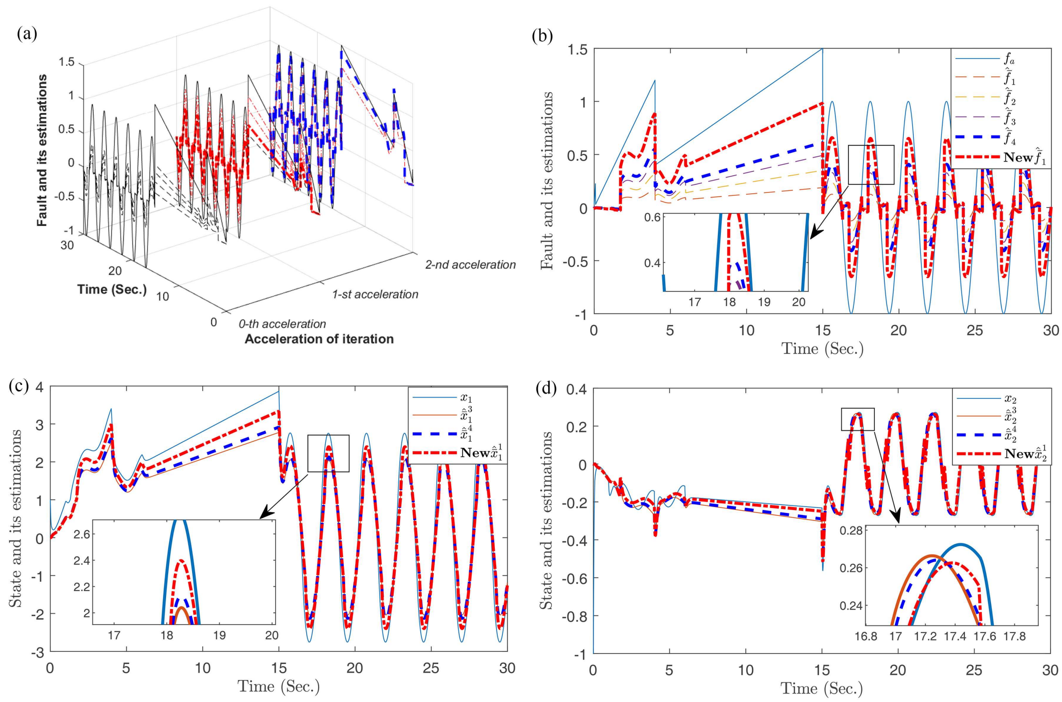

Figure 4 (Color online) Trajectories of fault reconstructions and comparison results in Example 2. (a) Trajectories of multiple acceleration fault reconstructions; (b) comparison between the conventional iterative learning law (blue) and the first accelerated iterative learning law (red) for fault reconstruction; (c) comparison between the conventional iterative learning law (blue) and the first accelerated iterative learning law (red) for the state estimation x_1; (d) comparison between the conventional iterative learning law (blue) and the first accelerated iterative learning law (red) for the state estimation x_2.

system matrices are expressed as follows:

$$A_1 = A_3 = \begin{bmatrix} -3.64 & 20 \\ -5 & -25 \end{bmatrix},\ A_2 = \begin{bmatrix} -0.04 & 20 \\ -5 & -25 \end{bmatrix},\ a_1 = \begin{bmatrix} -5.4 \\ 0 \end{bmatrix},\ a_2 = \begin{bmatrix} 0 \\ 0 \end{bmatrix},\ a_3 = \begin{bmatrix} 5.4 \\ 0 \end{bmatrix},$$

$$B_i = \begin{bmatrix} 9 \\ 9 \end{bmatrix},\ C_i = \begin{bmatrix} 1 & 1 \end{bmatrix},\ D_i = \begin{bmatrix} 0 \\ 5 \end{bmatrix},\ E_i = \begin{bmatrix} 1 & 0 \end{bmatrix},$$

where $i \in \boldsymbol{I}$, $\boldsymbol{I} = \{1, 2, 3\}$. From Theorem 1 associated with Algorithm 1, by employing the PWA iterative learning observer, the trajectories of actuator faults and the conventional-based, first-accelerated-based, and second-accelerated-based fault reconstructions are plotted in Figure 4(a). With the continued operation of the iterative accelerator, the estimation of the actuator fault can be obtained accurately via the PWA iterative learning observer after two consecutive accelerations. Moreover, from Corollary 1 associated with Algorithm 2, the trajectories of actuator faults, the system states, and their estimations are plotted in Figures 4(b)–(d), respectively. Figures 4(b)–(d) show that the convergence rates of the iterative estimation of both system state and system faults are improved significantly, and the first accelerated iterative learning law (red) can produce accurate estimation results faster than the conventional iterative learning law (blue).

5 Conclusion

This study investigated the fault reconstruction problem for a class of continuous-time PWA systems with actuator faults. First, a novel accelerated iterative learning law, which contains an iterative accelerator and a triggering condition, has been designed to resolve the issue of the "iteration bottleneck" existing in the conventional iterative learning law. Second, a novel learning law updating algorithm has been developed to describe the iterative procedure of augmented PWA estimation error systems against the region mismatch problem. Then, based on the designed fault reconstruction PWA iterative learning strategy, sufficient conditions for ensuring asymptotic stability with guaranteed $\mathcal{H}_\infty$ performance have been established for the augmented PWA estimation error system. Finally, the effectiveness and superiority of both the proposed accelerated iterative learning law and the learning law updating algorithms have been assessed using two examples, including a case study of a tunnel diode circuit system.

Acknowledgements This work was supported in part by National Natural Science Foundation of China (Grant Nos. 62222310, U1813201, 62473379), National Key Research and Development Program of China (Grant No. 2024YFB3310701), Research Fund for the Taishan Scholar Project of Shandong Province of China, Major Basic Research of Natural Science Foundation of Shandong Province (Grant No. ZR2024ZD38), and Japan Society for the Promotion of Science (Grant No. 21K04129).

References

1 Tian Y M, Chai Y, Feng L, et al. Fault estimator design based on an iterative-learning scheme according to the forgetting factor for nonlinear systems. Sci China Inf Sci, 2023, 66: 179201
2 Kazemi H, Yazdizadeh A. Fault reconstruction in a class of nonlinear systems using inversion-based filter. Nonlinear Dyn, 2016, 85: 1805–1814
3 Yan X G, Edwards C. Nonlinear robust fault reconstruction and estimation using a sliding mode observer. Automatica, 2007, 43: 1605–1614
4 Jia Q, Chen W, Zhang Y, et al. Robust fault reconstruction via learning observers in linear parameter-varying systems subject to loss of actuator effectiveness. IET Control Theor & Appl, 2014, 8: 42–50
5 Bahrami M, Naraghi M, Zareinejad M. Adaptive super-twisting observer for fault reconstruction in electro-hydraulic systems. ISA Trans, 2018, 76: 235–245
6 Zhou B, Shi Y. Prescribed-time stabilization of a class of nonlinear systems by linear time-varying feedback. IEEE Trans Automat Contr, 2021, 66: 6123–6130
7 Yang Y N, Jiang H X, Hua C C, et al. Finite-time composite learning control for nonlinear teleoperation systems under networked time-varying delays. Sci China Inf Sci, 2024, 67: 162203
8 Xie R M, Xu S Y. Fixed-time stabilization of output-constrained stochastic high-order nonlinear systems. Sci China Inf Sci, 2024, 67: 140201
9 Zhang L, Shi P. l_2-l_∞ model reduction for switched LPV systems with average Dwell time. IEEE Trans Automat Contr, 2008, 53: 2443–2448
10 Zou W, Ahn C K, Xiang Z. Analysis on existence of compact set in neural network control for nonlinear systems. Automatica, 2020, 120: 109155
11 Ning Z, Cai B, Weng R, et al. Nonsynchronized state estimation for fuzzy Markov jump affine systems with switching region partitions. IEEE Trans Cybern, 2022, 52: 2430–2439
12 Hassibi A, Boyd S. Quadratic stabilization and control of piecewise-linear systems. In: Proceedings of the American Control Conference, Philadelphia, 1998. 3659–3664
13 Ning Z, Feng G, Yin X. Asynchronous quantized control of piecewise-affine systems. IEEE Trans Automat Contr, 2024, 69: 503–510
14 Ning Z, Zhang L, Feng G, et al. Observation for Markov jump piecewise-affine systems with admissible region-switching paths. IEEE Trans Automat Contr, 2021, 66: 4319–4326
15 Zhu Y, Zheng W X. Multiple Lyapunov functions analysis approach for discrete-time-switched piecewise-affine systems under Dwell-time constraints. IEEE Trans Automat Contr, 2020, 65: 2177–2184
16 Zhu Y, Xu N, Chen X, et al. H_∞ control for continuous-time Markov jump nonlinear systems with piecewise-affine approximation. Automatica, 2022, 141: 110300
17 Zhang L, Ning Z, Zheng W X. Observer-based control for piecewise-affine systems with both input and output quantization. IEEE Trans Automat Contr, 2017, 62: 5858–5865
18 Wang M, Qiu J, Yan H, et al. Data-driven control for discrete-time piecewise affine systems. Automatica, 2023, 155: 111168
19 Ma A, Li D, Xi Y. Distributed MPC based on robustly controllable sets for PWA systems. Automatica, 2023, 154: 111078
20 Liu T, Buss M. Output feedback model reference adaptive control of piecewise affine systems with parameter convergence analysis. IEEE Trans Automat Contr, 2022, 67: 3707–3714
21 Vaezi M, Izadian A. Piecewise affine system identification of a hydraulic wind power transfer system. IEEE Trans Contr Syst Technol, 2015, 23: 2077–2086
22 Buire J, Colas F, Dieulot J Y, et al. Confidence level optimization of DG piecewise affine controllers in distribution grids. IEEE Trans Smart Grid, 2020, 10: 6126–6136
23 Sun X, Wang Y, Quan Z, et al. DYC design for autonomous distributed drive electric vehicle considering tire nonlinear mechanical characteristics in the PWA form. IEEE Trans Intell Transp Syst, 2023, 24: 11030–11046
24 Li L, Ding S X, Qiu J, et al. An optimal fault detection approach for piecewise affine systems via diagnostic observers. Automatica, 2017, 85: 256–263
25 Han J, Zhang H, Wang Y, et al. Fault estimation and fault-tolerant control for switched fuzzy stochastic systems. IEEE Trans Fuzzy Syst, 2018, 26: 2993–3003
26 Liu X, Gao X, Han J. Distributed fault estimation for a class of nonlinear multiagent systems. IEEE Trans Syst Man Cybern Syst, 2020, 50: 3382–3390

27 Alessandri A, Boem F, Parisini T. Model-based fault detection and estimation for linear time invariant and piecewise affine systems by using quadratic boundedness. In: Proceedings of IEEE Conference on Decision and Control, Miami, 2019. 5562–5567

28 Richter J H, Heemels W P M H, van de Wouw N, et al. Reconfigurable control of piecewise affine systems with actuator and sensor faults: stability and tracking. Automatica, 2011, 47: 678–691

29 Tzeng K S, Tzeng D C, Chen J S. An enhanced iterative learning control scheme using wavelet transform. IEEE Trans Ind Electron, 2005, 52: 922–924

30 Cao Z, Durr H B, Ebenbauer C, et al. Iterative learning and extremum seeking for repetitive time-varying mappings. IEEE Trans Automat Contr, 2017, 62: 3339–3353

31 Yang L, Li Y, Huang D, et al. Spatial iterative learning control for robotic path learning. IEEE Trans Cybern, 2022, 52: 5789–5798

32 Pakshin P, Emelianova J, Emelianov M, et al. Passivity based stabilization of repetitive processes and iterative learning control design. Syst Control Lett, 2018, 122: 101–108

33 Liu J, Zheng Y, Chen Y Q. Monotonically convergent iterative learning control by time varying learning gain revisited. Automatica, 2023, 157: 111259

34 Xu S, Dai H, Feng L, et al. Fault estimation for switched interconnected nonlinear systems with external disturbances via variable weighted iterative learning. IEEE Trans Circuits Syst II, 2023, 70: 2011–2015

35 Chen L, Zhu Y, Wu F, et al. Fault estimation observer design for Markovian jump systems with nondifferentiable actuator and sensor failures. IEEE Trans Cybern, 2023, 53: 3844–3858

36 Zhu Y, Xu N, Wu F, et al. Fault estimation for a class of Markov jump piecewise-affine systems: current feedback based iterative learning approach. IEEE CAA J Autom Sin, 2024, 11: 418–429

37 Wang R, Zhuang Z, Tao H, et al. Q-learning based fault estimation and fault tolerant iterative learning control for MIMO systems. ISA Trans, 2023, 142: 123–135

38 Feng G. Controller design and analysis of uncertain piecewise-linear systems. IEEE Trans Circuits Syst I, 2002, 49: 224–232

39 Johansson M, Rantzer A. Computation of piecewise quadratic Lyapunov functions for hybrid systems. IEEE Trans Automat Contr, 1998, 43: 555–559

40 Iervolino R, Tangredi D, Vasca F. Lyapunov stability for piecewise affine systems via cone-copositivity. Automatica, 2017, 81: 22–29

41 Yin S, Yang H, Kaynak O. Sliding mode observer-based FTC for Markovian jump systems with actuator and sensor faults. IEEE Trans Automat Contr, 2017, 62: 3551–3558

42 Sun Y, Yu J, Li Z. Event-triggered finite-time robust filtering for a class of state-dependent uncertain systems with network transmission delay. IEEE Trans Circuits Syst I, 2019, 66: 1076–1089